International Journal of Thin Films Science and Technology

http://dx.doi.org/10.18576/ijtfst/100107

Effects of Ni - Doping on the Characterization of Nanostructured CdS Thin Films

Kameran Yasseen Qader[1], *Esraa Hassn Hadi*[1], *Nadir Fadhil Habubi*[1], *Sami Salman Chiad*[1], *M. Jadan*[2,3], *Jihad S. Addasi*[4,*]

[1]Department of Physics, College of Education, Mustansiriyah University, Baghdad, Iraq
[2]Department of Physics, College of Science, Imam Abdulrahman Bin Faisal University, P.O. Box 1982, 31441 Damma/, Saudi Arabia
[3]Basic and Applied Scientific Research Center, Imam Abdulrahman Bin Faisal University, P.O. Box 1982, 31441 Dammam, Saudi Arabia
[4]Department of Applied Physics, College of Science, Tafila Technical University, 66110 Tafila, Jordan

Received: 21 Feb. 2020, Revised: 22 Mar. 2020, Accepted: 24 Mar. 2020.
Published online: 1 Jan. 2021

Abstract: Effect of nickel doping was investigated on doped CdS films by spray pyrolysis technique and examined by XRD, AFM, and UV-VIS spectroscopy. The increasing of Ni doping ratio improve (020) preferential orientation. XRD analysis confirmed the CdS nanostructure for all samples. The crystallite size for pure CdS showed an increase from 19.98 nm to 27.04 nm on doping, whereas the strain (%) parameter was decreased from 25.0 to 13.3.
AFM images offer a decrease in roughness from 6.5 nm to 3.48 nm with Ni – 4% content. Transmittance was exceeding 70% in the visible range by Ni content. Also, the bandgap was decreased from 2.4 to 2.3 eV with the increment of Ni content.

Keywords: CdS, spray pyrolysis, surface morphology, Ni doping, bandgap.

1 Introduction

Cadmium sulfide group II-VI semiconductors, wide bandgap, high, transparency and electron affinity [1-3]. Owing to these characterizations it can be act a window layer in solar cells [4-6]. Besides it can be used as light emitting diodes [7], photonic devices [8–10], photoconductive sensors [11], environmental pollution control [12], photocatalysis [13-19]. The importance of Ni doping lies in its ability to enhance the performance of electrical properties of CdS, Besides the Ni atoms is a favorable material for promoting the efficiency of CdS films in photovoltaic devices. Yahia et al. [20] studied the physical properties of CdS:Ni showing the bandgap of 2.49 - 2.2 with Ni content. Mahdi et al. [21] prepared CdS:Ni via sol-gel method their work reached at the increase of bandgap with Ni content. Kumar et al. [22] found that by increasing Ni content there is a shift toward short wavelength. Jothi et al [23] try to tune the properties of CdS by Ni content, a shift toward long wavelength were noticed.

This paper is focused on the preparation of CdS:Ni and study their characterization using a costless and simple technique with nearly homogeneity films, which is chemical spray pyrolysis.

2 Experimental works

CdS:Ni films were deposited using CSP method. 0.01 M of Cd [$C_4H_6CdO_4$] and 0.01 M thiourea [CH_4N_2S] as cadmium and sulphur source respectively. Nickel chloride [$NiCl_3$] was used for Ni doping with different contents (2, 4 at % Ni).

Substrate temperature was preserved at 400 ° C through deposition process. Carrier gas was Nitrogen. Deposition rate was 6 mL/min, sprayer rate was 8 s lasted by 50 Sec to prevent high cooling. Space among substrate and nozzle was kept at 30 cm. The structure of nanostructured CdS:Ni were analyzed by X-ray diffraction via X-ray diffractometer using CuKα radiation (λ=1.54012 Å) in the range of 20 ° – 60 ° (2θ) at scanning rate of 0.05 °/min. Transmittance spectra were utilized employing UV-VIS spectrophotometer (Lambda 750 Perkin Elmer).

*Corresponding author E-mail: addasijihad@gmail.com

3 Results and Discussion

Fig. 1 offers XRD patterns of the deposited films, the characteristic peaks (011), (020), (121), and (220) corresponding to diffraction 2θ = 31.79 º, 36.99 º, 53.47 º and 66.22 º showed good crystalline nature of prepared samples and well matched with cubic zinc-blende (JCPDS 43-0985). By increasing Ni concentration, a shift in 2θ the position toward the lower from 36.99 º for undoped film to 36.65 º for CdS: 4% Ni films and this could be assigned to the replacement of CdS ions by Ni ions.

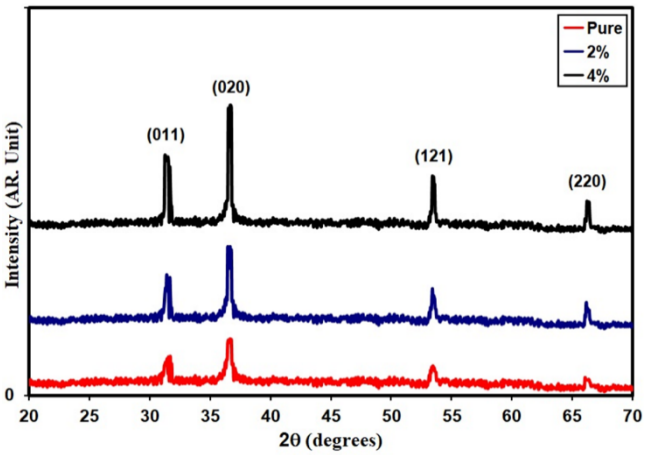

Fig.1:XRD-patterns crystalline size of the prepared films.

The crystallite size (D) was obtained from the highest intensity peaks utilizing Scherrer's equation [22, 23]:

$$D = \frac{0.9\lambda}{\beta\cos\theta} \quad (1)$$

Where λ is the wavelength of the X-rays (1.5406 Å), β and θ are (FWHM) and Bragg's angle respectively. The crystalline size has been found to vary from 19.98 to 27.04 nm with Ni concentration, that is the Ni doping enhance the crystallization of the chalcogenide as listed in Table 1, 2.

Table 1. Grain size, optical bandgap of the prepared films.

Samples	(hkl) Plane	2 θ (º)	Opt. band gap (eV)	Grain size (nm)
CdS pure	020	36.99	2.40	19.98
CdS: 2% Ni	020	36.75	2.35	24.64
CdS: 4% Ni	020	36.65	2.3	27.04

Other structural parameters such as dislocation density δ and strain ε are also evaluated, Table 2. δ gives number of defects, the values of δ and ε listed in Table 2 show the structural parameters estimated from [24, 25]:

$$\delta = \frac{1}{D^2} \quad (2)$$

$$\varepsilon = \frac{\beta\cos\theta}{4} \quad (3)$$

Table 2. Structural parameters of the prepared films.

Samples	FWHM (º)	Disloc. Density ($\times 10^{14}$) (lines/m^2)	Strain ($\times 10^{-4}$)
CdS pure	0.42	25.0	17.3
CdS: 2% Ni	0.34	16.4	14.0
CdS: 4% Ni	0.31	13.3	12.8

Fig. 2 represents β, D, δ and ε versus Ni content. It can be seen that the value of δ and ε were decrease as Ni dopant increase, which agree with D that when these parameters decrease there will be an increase in D.

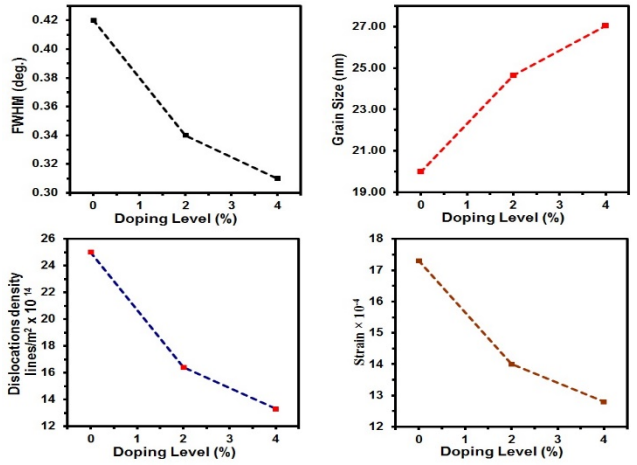

Fig.2: FWHM (a) Grain size (b) Dislocation (c) Strain (d) of the prepared films.

Atomic force microscope AFM micrographs and their roughness analysis of prepared CdS:Ni films are demonstrated in Fig. 3 a1, b1, and c1. The 3-D images and grain size distribution are given in, they exhibit spherical nano-grains ranged from 87.36 nm for pure Ni to 65.03 nm for 4% Ag doped Ni. The change in surface morphology ranged from 6.50 to 3.48 nm with the increase of silver doping. By increasing Ni doping, the decrease in average surface roughness was due to the reduction in grain size. The influence of Ni doping on AFM parameters namely grain size (D), surface roughness (Ra) and root root-mean-square (Rrms) are shown in Fig. 3 a3, b3, and c3 respectively. Table 3 represents the values of AFM parameters.

The transmittance of CdS:Ni films is shown in Fig. 4 A decrease in transmittance from 80% to 45% at doping concentration 4 wt% was noticed. The absorption coefficient (α) of films was specified by equation [26, 27,

and 28]:

$$\alpha = \frac{\ln (1/T)}{d} \qquad (4)$$

where d is film thickness. Fig. 5 represents α that assures direct transition.

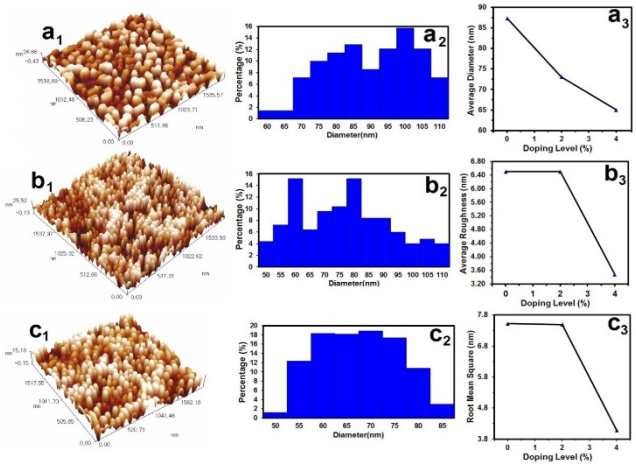

Fig. 3: AFM images of the prepared films (a_1, b_1 and c_1), granularly distributed (a_2, b_2 and c_2) and variation of AFM parameters via doping (a_3, b_3 and c_3).

Table 2. AFM parameters of the deposited films.

Samples	Average Particle size (nm)	Roughness Average (nm)	R. M. S. (nm)
CdS pure	87.36	6.50	7.52
CdS: 2% Ni	73.04	6.50	7.49
CdS: 4% Ni	65.03	3.48	4.08

The optical bandgap was evaluated from next relation [29, 30, and 31]:

$$\alpha h\upsilon = G(h\upsilon - E_g)^2 \qquad (5)$$

where α, hν, G and E_g are absorption coefficient, photon energy, proportional constant and energy gap respectively.

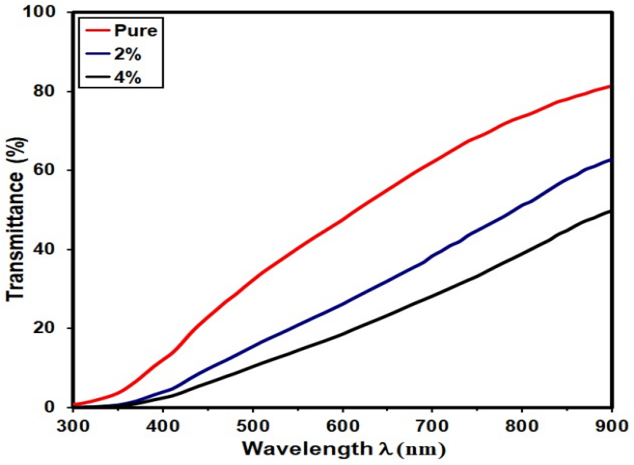

Fig. 4: Transmittance for the prepared films.

By using of x-axis intersection of αhν versus hν plots, the optical energy gap was determined as shown in Fig. 6 Eg values decreased from 2.4 to 2.3 eV with the increment of Ni doping level, which was agreed with the XRD the data obtained by XRD.

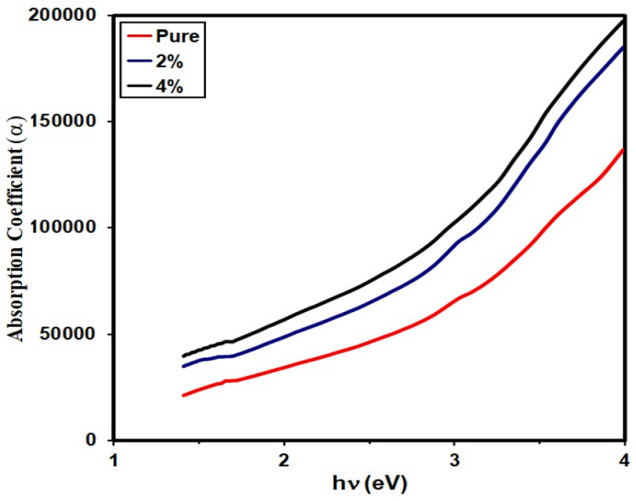

Fig. 5: α Vs hν of the prepared thin films.

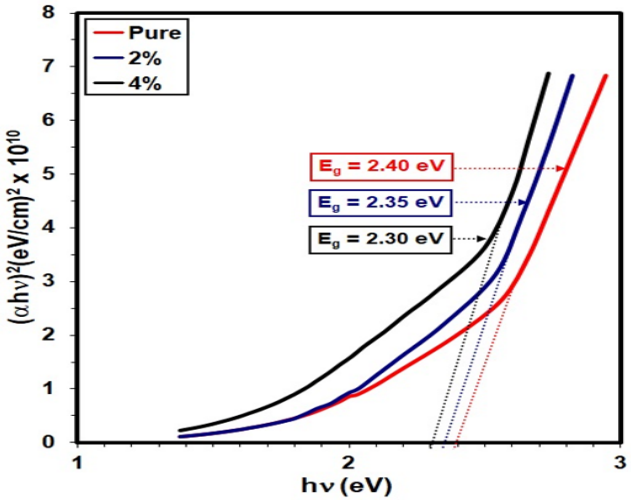

Fig. 6: $(\alpha h\nu)^2$ Vs hν of the prepared thin films.

4 Conclusions

Ni-doped CdS films were deposited using spray pyrolysis. The increase of Ni content improve the (020) preferential orientation. XRD analysis confirmed the CdS nanostructure for all samples. The crystallite size for pure CdS shows an increase from 19.98 nm to 27.04 nm on doping, whereas the strain (%) parameter decrease from 25.0 to 13.3, AFM images of the films display changes in morphology with a decrease in roughness from 6.5 nm to 3.48 nm with Ni - 4% doping. The optical bandgap changes with Ni as 2.4–2.3 eV.

Acknowledgement

Authors would appreciate Mustansiriyah University for their support.

References

[1] D. Aldakov, A. Lefrancois and P. Reiss, Journal of Materials Chemistry., **C1 24**, 3756-3776 (2013).

[2] R. Yousefi, F. Jamali-Sheini and A.K. Zak, Metal Chalcogenide Nanostructures for Renewable Energy Applications., 189-232 (2014).

[3] A. Rmili, F. Ouachtari, A. Bouaoud, A. Louardi, T. Chtouki, B. Elidrissi and H.Erguig, Journal of Alloys and Compounds 557, 53-59 (2013).

[4] A. Ashour, J. Optoel. Adv. Mater. 8, 1447-1451 (2006).

[5] M. Acevedo, Sol. Energy., **80**, 675-681 (2006). [CrossRef]

[6] S. Shirakata and K. Ohkubo, Sol. Energy Mater. Sol. Cells 93, 988-992 (2009). [CrossRef]

[7] H. Murai, T. Abe, J. Matsuda and H. Sato, Appl. Surf. Sci. 244, 351-354 (2005).

[8] B. Ullrich, D. M. Bagnall, H. Sakai and Y. Segawa, Solid State Commun., **109**, 757-760 (1999).

[9] S. A. Vanalakar, S. S. Mali, M. P. Suryavanshi and P. S. Patil, Dig. J. Nanomater. Biostruct., **5**, 805-810 (2010).

[10] V. Popescu, H. I. Nascu and E. Darvasi, J. Optoelectron. Adv. Mater., **8**, 1187-1193 (2006).

[11] S. -G. Hur, E. -T. Kim, J. -H. Lee, G. -H. Kim and S. -G. Yoona, J. Vac. Sci. Technol., **B 26**, 1334-1337 (2008).

[12] Y. V. Marathe and V. S. Shrivastava, Adv. Appl. Sci. Res., **2**, 295-301 (2011).

[13] J. Jin, J. Yu, G. Liu and P. K. Wong, J. Mater. Chem. A 1, 10927-10934 (2013).

[14] N. Zhang, M. Yang, Z. Tang and Y. Xu, J. Catal., **303**, 60-69 (2013).

[15] L. Long, X. Yu, L. Wu, J. Li and X. Li, Nanotechnology 25, 035603 (2014).

[16] J. Fu, B. Chang, Y. Tian, F. Xi and X. Dong, J. Mater. Chem., **A 1**, 3083-3090 (2013).

[17] M. Moriya, T. Minegishi, H. Kumagai, M. Katayama, J. Kubota and K. Domen, J. Am. Chem. Soc., **135**, 3733-3735 (2013).

[18] S. R. Lingampalli, U. K. Gautam and C. N. R. Rao, Energy Environ. Sci., **6**, 3589-3594 (2013).

[19] K. Zhang, D. Jing, C. Xing and L. Guo, Int. J. Hydrog. Energy., **32**, 4685-4691 (2007).

[20] I. S. Yahia, I. M. El Radaf, A. M. Salem and G. B. Sakr, Journal of Alloys and Compounds., **776**, 1056-1062 (2019).

[21] H. S. Mahdi, A. Parveen and A. Azam, Materials Today: Proceedings., **5**, 20636-20640 (2018).

[22] A. A. Khadayeir, E. S. Hassan, S. S. Chiad, N. F. Habubi, Kh. H. Abass, M. H. Rahid, T. H. Mubarak, M. O. Dawod and I. A. Al-Baidhany, J. of Physics: Conference Series., **1234**, 012014 (2019).

[23] S. S. Chiad and T. H. Mubarak, Int. J. of Nanoelectronics and Materials., **13(2)**, 221-232 (2020).

[24] E. S. Hassan, T. H. Mubarak, S. S. Chiad, N. F. Habubi, A. A. Khadayeir, M. O. Dawood and I. A. Al-Baidhany, IOP Conf. Series: Journal of Physics: Conf. Series., **1294**, 022008 (2019).

[25] N. N. Jandow, N. F. Habubi, S. S. chiad, I. A. Al-Baidhany and M. A. Qaeed, Int. J. of Nanoelectronics and Materials., **12(1)**, 1-10 (2019).

[26] A. Sh. Alkelaby, Kh. H. Abass, T. H. Mubarak, N. F. Habubi, S. S. Chiad and I. Al-Baidhany, J. of Global Pharma Technology., **11(4)**, 347-352 (2019).

[27] S. S. Chiad, H. A. Noor, O. M. Abdulmunem and N. F. Habubi, IOP Conf. Series: J. of Physics: Conf. Series., **1362**, 012115 (2019).

[28] S. S. Chiad, Kh. H. Abass, T. H. Mubarak, N. F. Habubi, M. Kh. Mohammed and A. A. Khadayeir, J. of Global Pharma Technology., **11(4)**, 369-374 (2019).

[29] A. A. Khadayeir, Kh. H. Abass, S. S. Chiad, M. Kh. Mohammed, N. F. Habubi, T. Kh. Hameed and I. A. Al-Baidhany, J. of Engineering and Applied Sciences., **13(22)**, 9689-9692 (2018).

[30] M. O. Dawood, S. S. Chiad, A. J. Ghazai, N. F. Habubi and O. M. Abdulmunem, AIP Conference Proceedings., **2213 (1)**, 020102 (2020).

[31] S. S. Chiad, K. H. Abass, T. H. Mubarak, N. F. Habubi, M. K. Mohammed and A. A. Khadayeir, J. of Global Pharma Technology., **11(4)**, 369-375 (2019).